Bootstrapping (Ultrafast) Photoionization Dynamics

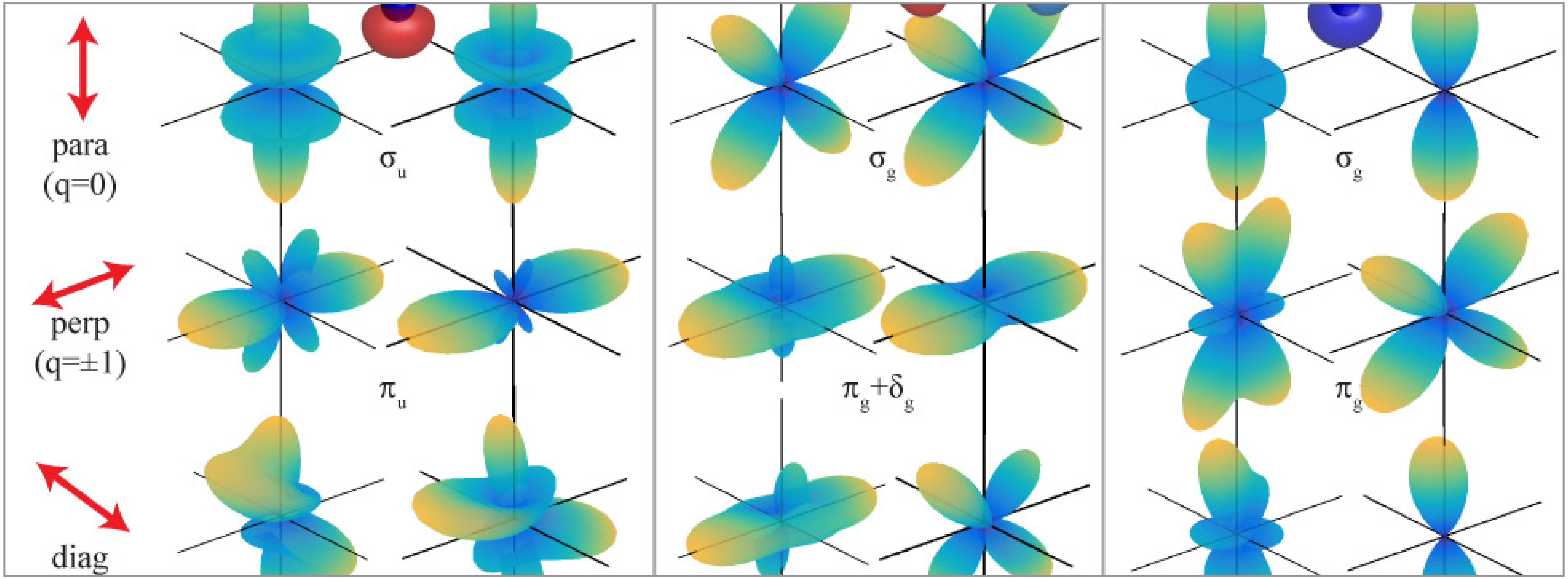

Paul Hockett
femtolab.ca
National Research Council of Canada, Ottawa

Available via Figshare, DOI: 10.6084/m9.figshare.5645509

photoionization interferometry

Photoionization is an interferometric process, in which multiple paths can contribute to the final continuum photoelectron state.

(1) Intrinsic: interferences between final (continuum) states - photoionization dynamics.

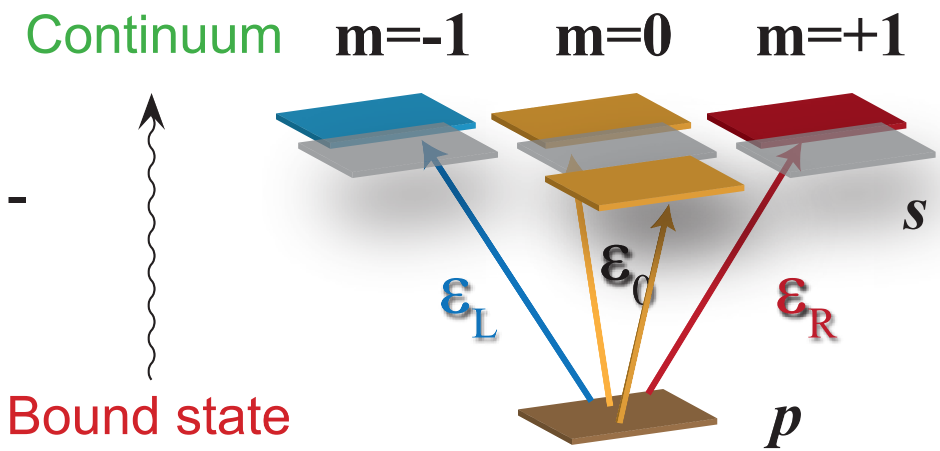

(2) Extrinsic/dynamic: additional pathways due to, e.g., prepared wavepacket, control fields, etc. etc.

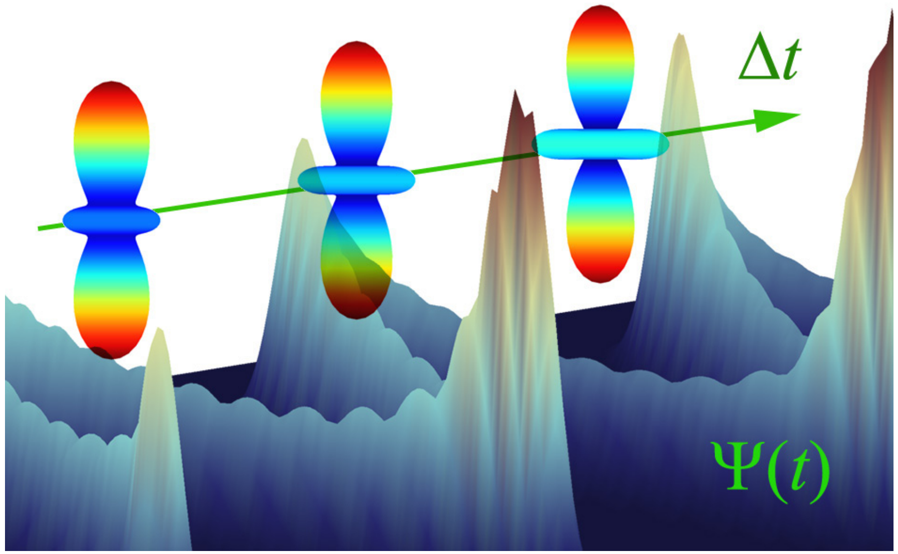

For an early discussion along these lines, see:
Cohen, H., & Fano, U. (1966).
Interference in the Photo-Ionization of Molecules.
Physical Review, 150(1), 30–33.
http://doi.org/10.1103/PhysRev.150.30

femtolab.ca

photoionization interferometry

Photoionization is an interferometric process, in which multiple paths can contribute to the final continuum photoelectron state.

(1) Intrinsic: interferences between final (continuum) states - photoionization dynamics.

(2) Extrinsic/dynamic: additional pathways due to, e.g., prepared wavepacket, control fields, etc. etc.

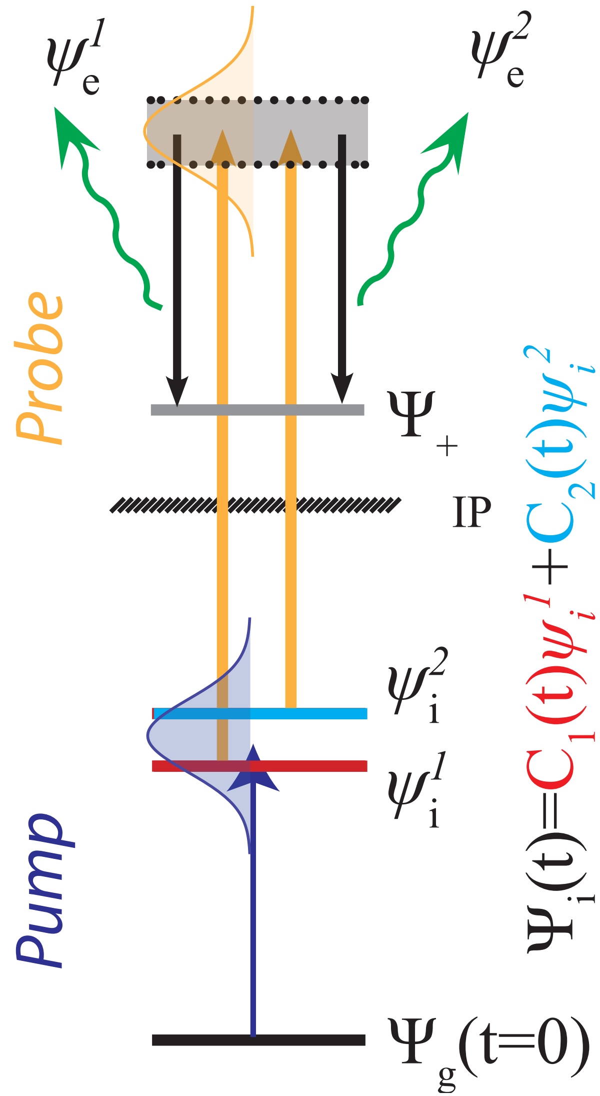

femtolab.ca

photoelectron metrology

Photoelectron spectroscopy with a focus on (quantitative) photoionization dynamics.

With sufficient experimental information content, photoionization matrix elements (magnitudes & phases) can be retrieved.

cf.

- “complete” photoionization and scattering experiments
- quantum process & state tomography

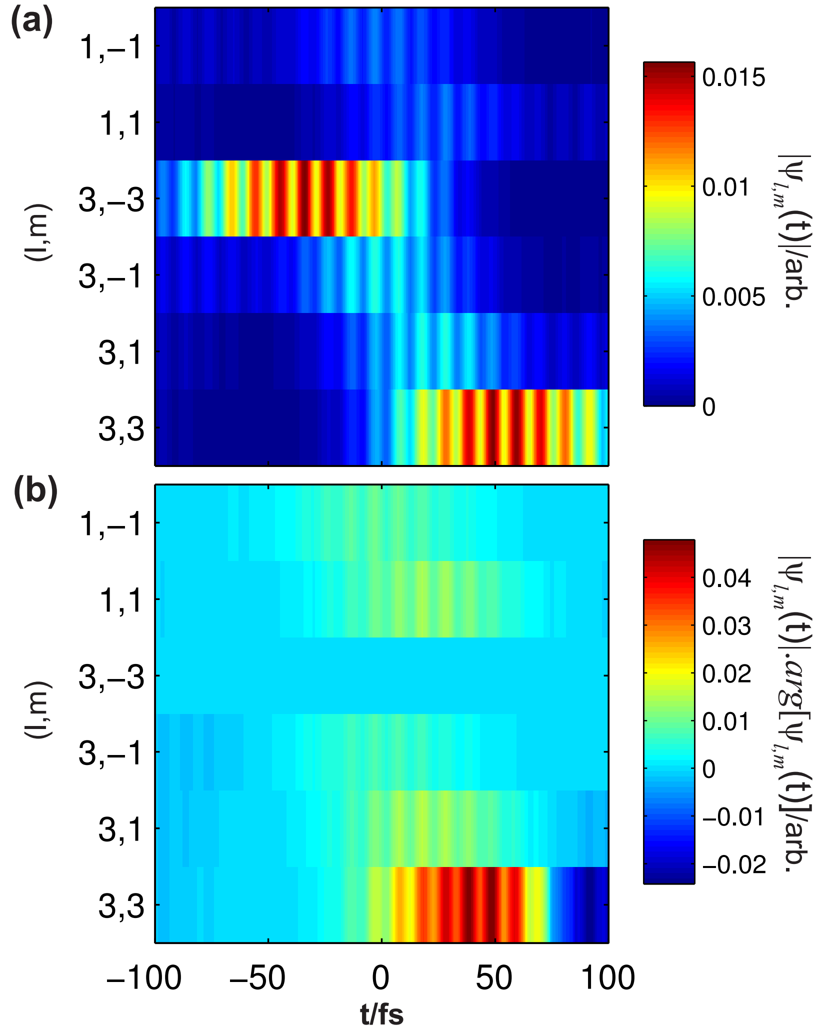

Hockett, P., Wollenhaupt, M., & Baumert, T. (2015).
Coherent control of photoelectron wavepacket angular interferograms.
Journal of Physics B: Atomic, Molecular and Optical Physics, 48(21), 214004.
http://doi.org/10.1088/0953-4075/48/21/214004

matrix element reconstruction

Requires:
(1) A phase-sensitive observable... photoelectron angular distributions (PADs) are angle-resolved photoelectron interferograms.

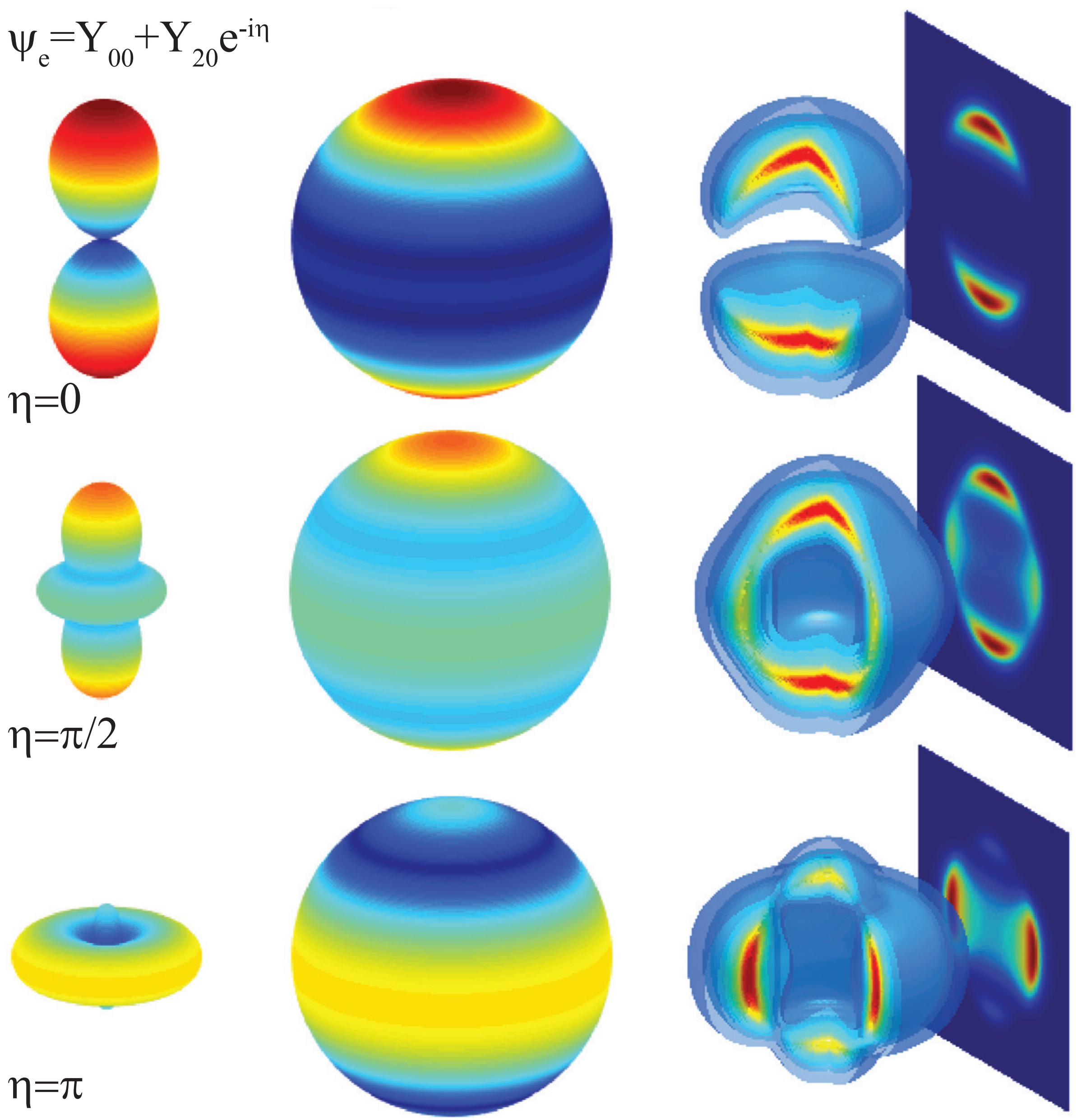

femtolab.ca

matrix element reconstruction

Requires:
(1) A phase-sensitive observable... photoelectron angular distributions (PADs) are angle-resolved photoelectron interferograms.

(2) Reconstruction/retrieval technique for the system properties of interest (matrix elements, density matrix etc.).

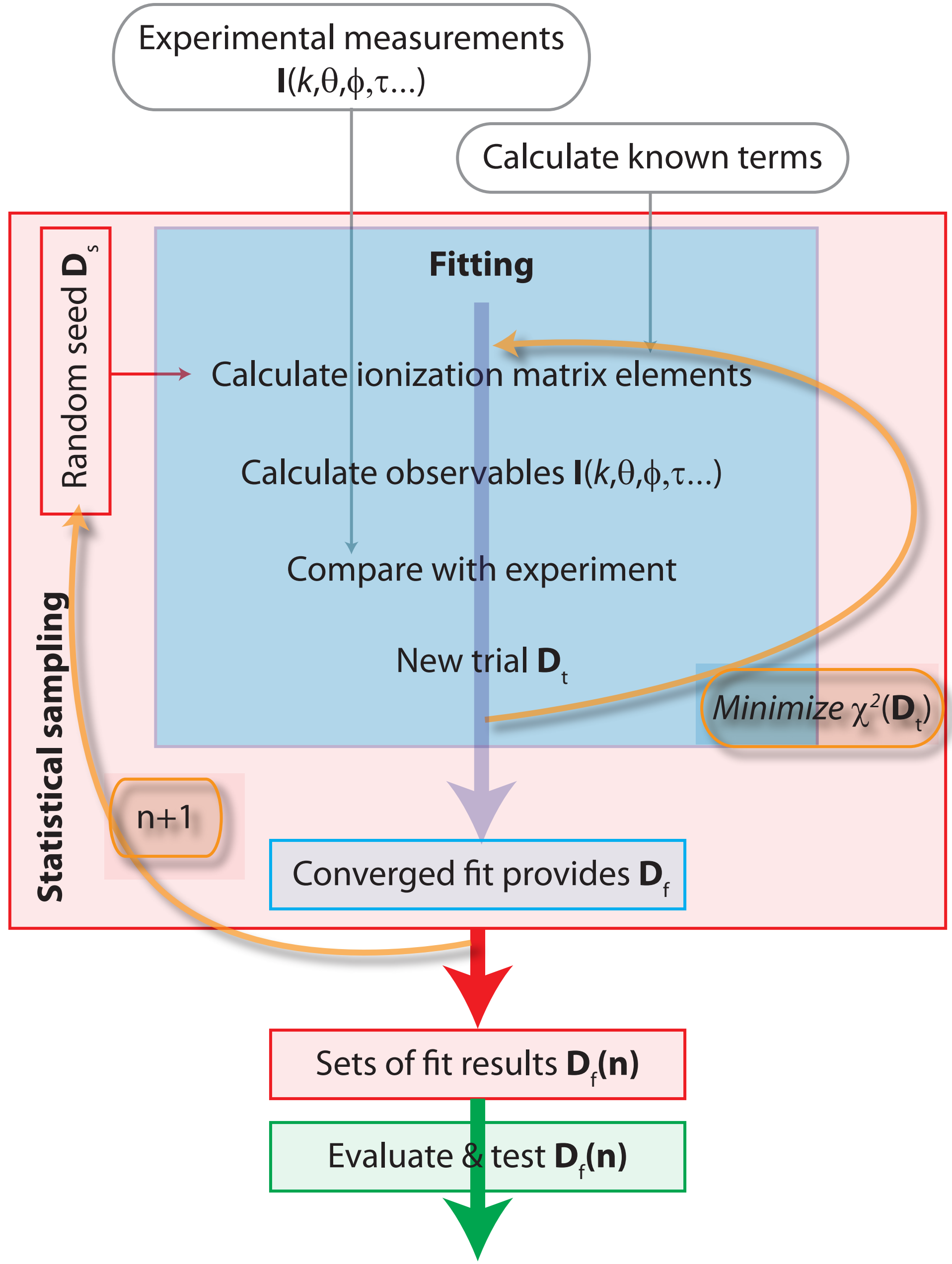

femtolab.ca

Bootstrapping to the Molecular Frame with Time-domain Photoionization Interferometry

[Alt. title: *Molecular Frame Reconstruction Using Time-Domain Photoionization Interferometry*]

Claude Marceau, Varun Makhija, Dominique Platzer, A. Yu. Naumov, P. B. Corkum, Albert Stolow, D. M. Villeneuve and Paul Hockett
Phys. Rev. Lett., 119(8), 83401. http://doi.org/10.1103/PhysRevLett.119.083401

arXiv 1701.08432 (https://arxiv.org/abs/1701.08432).

Docs, data & code repository (figshare)

DOI: 10.6084/m9.figshare.4480349
https://dx.doi.org/10.6084/m9.figshare.4480349.

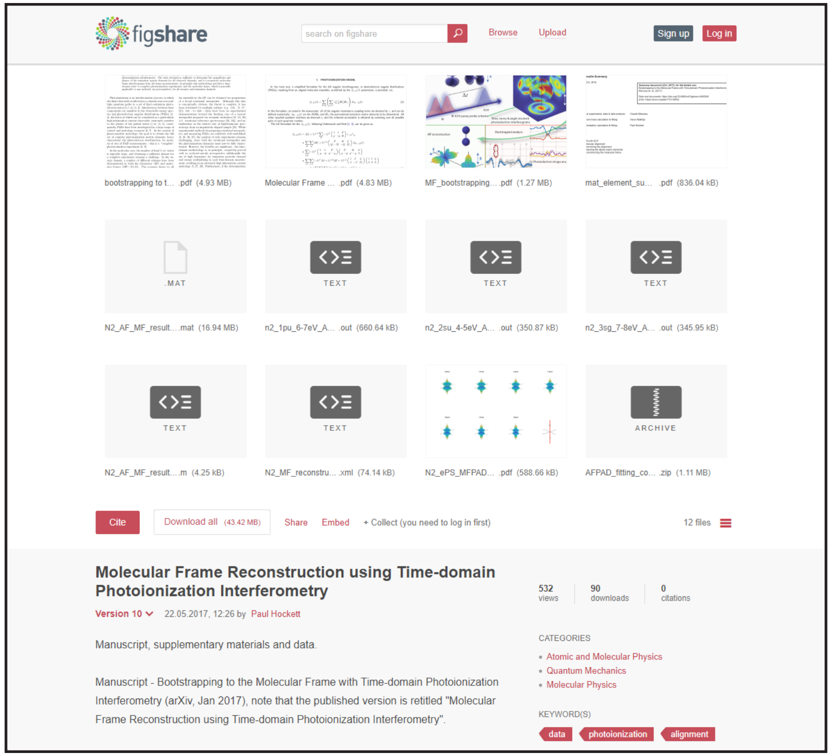

femtolab.ca

bootstrapping concept

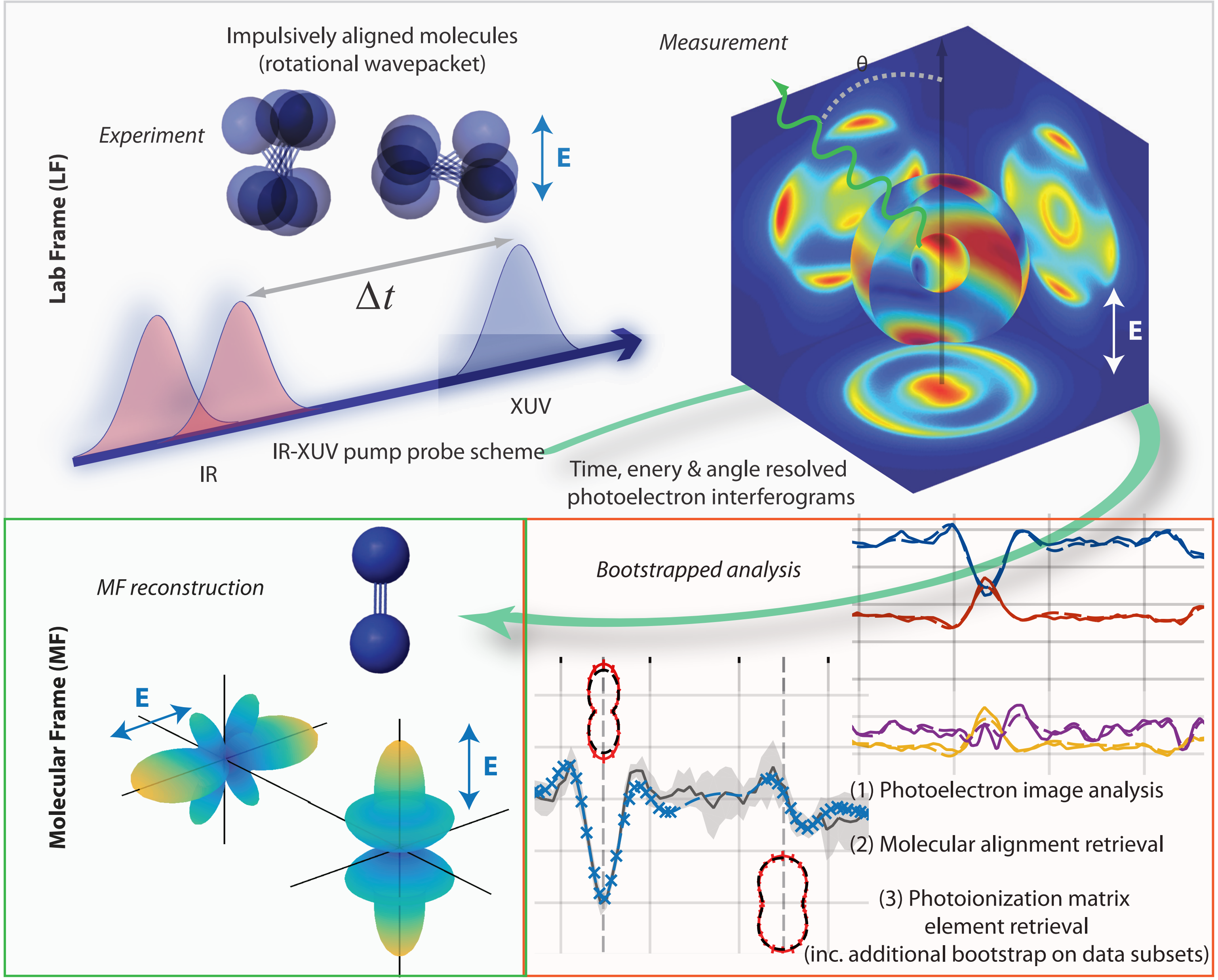

femtolab.ca

bootstapping scheme

Pump-probe scheme

$$|\Psi_g\rangle \overset{E_1^{IR}(t)+E_2^{IR}(t)}{\longrightarrow} |\Psi_g(t)\rangle \overset{E^{XUV}(t)}{\longrightarrow} |\Psi_+^\Gamma;\Psi_e^\Gamma(k)\rangle$$

$$\downarrow$$

Pump: rotational wavepacket for geometric control

$$|X^1\Sigma_g^+\rangle|v_X\rangle|J_X M_X\rangle \overset{E_1^{IR}(t)+E_2^{IR}(t)}{\longrightarrow} |X^1\Sigma_g^+\rangle|v_X\rangle \sum_{J_X M_X} C_{J_X M_X}(t)|J_X M_X\rangle$$

$$\downarrow$$

Ensemble alignment: $P(\theta,\phi,t) = \sum_{K,Q} A_{K,Q}(t) Y_{K,Q}(\theta,\phi)$

Probe: photoelectron + photoion products

$$\overset{E^{XUV}(t)}{\longrightarrow} |\mathbf{k},\Gamma l\lambda m\rangle|\Gamma\rangle|v_\Gamma\rangle \sum_{J_\Gamma M_\Gamma} C_{J_\Gamma M_\Gamma}(t)|J_\Gamma M_\Gamma\rangle$$

femtolab.ca

experiment

- High harmonic generation, driven with 400 or 267nm.
- Single or multiple IR pulses for impulsive molecular align-ment (rotational wavepacket).

VMI for photoelectron measurements

High harmonic generation

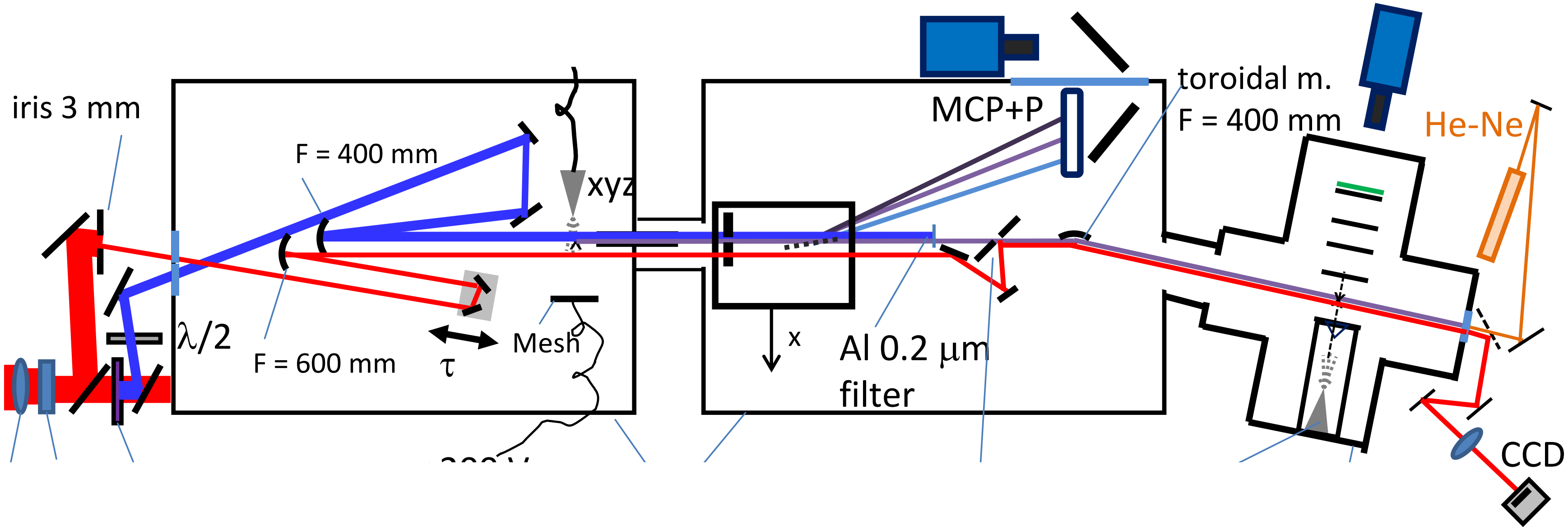

Claude Marceau & Dominique Platzer, NRC Jaslab (2016)

femtolab.ca

(1) empirical analysis

Measurements - time, energy and angle-resolved photoelectron yields.

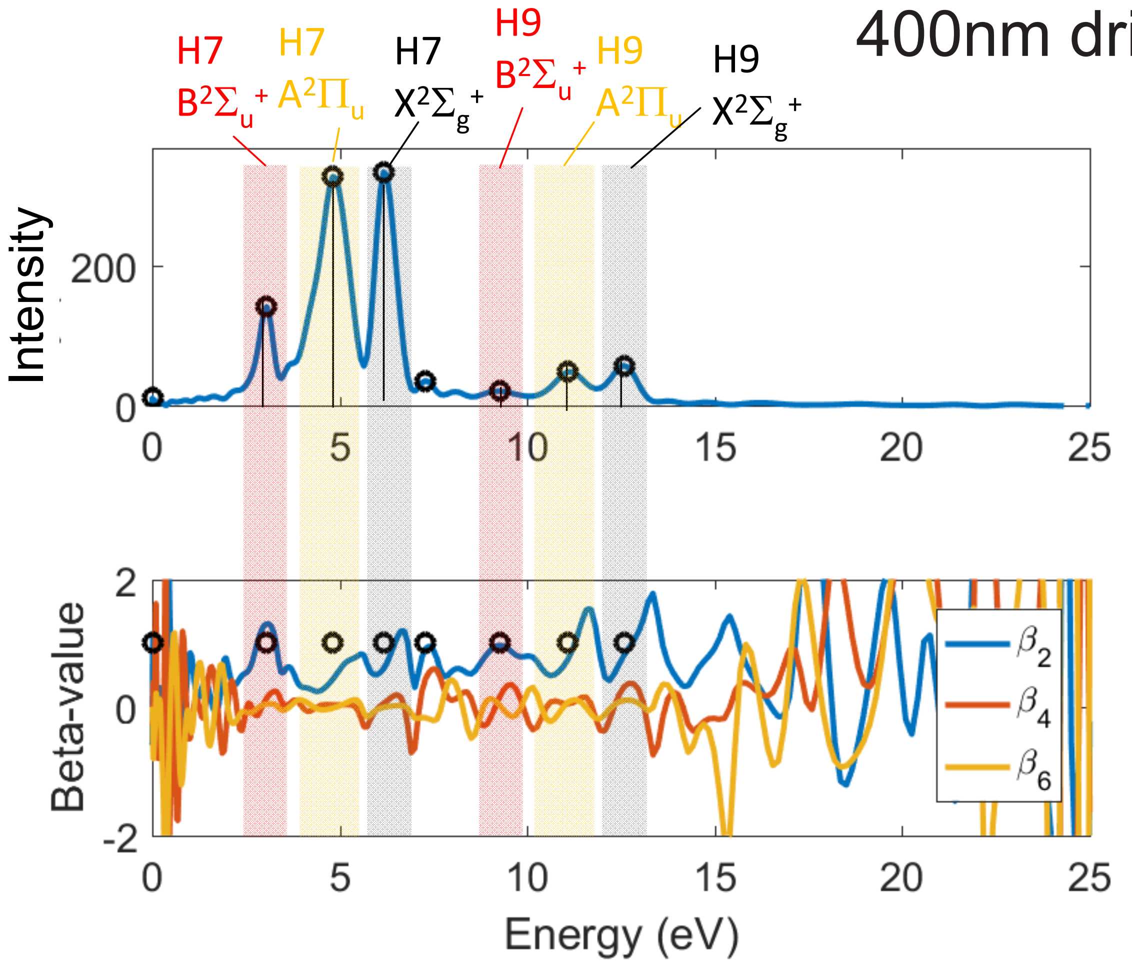

400nm driving field

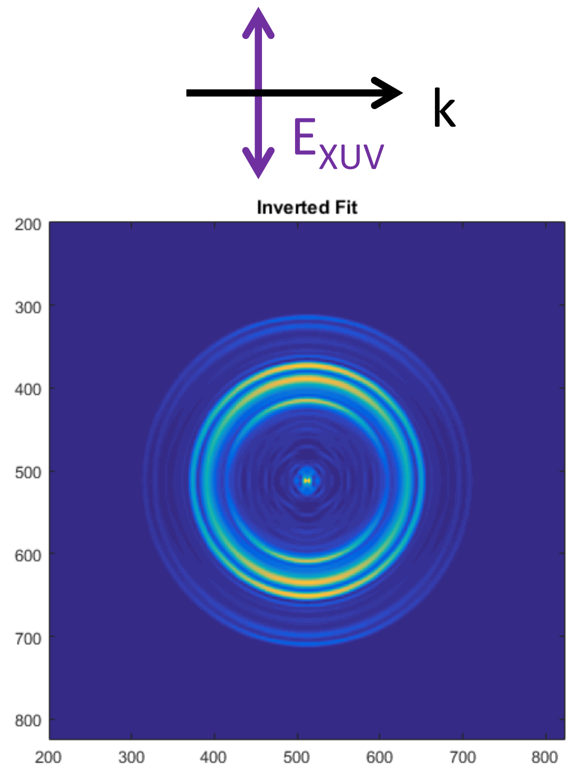

$$I(\theta,\phi;k,t) = \sum_{L=0}^{2l_{max}} \sum_{M=-L}^{L} \beta_{LM}(k,t) Y_{LM}(\theta,\phi)$$

Anisotropy parameters   Spherical harmonics

femtolab.ca

(1) N_2 dataset

- 267nm driving field
- Two-pulse IR rotational wavepacket preparation
- 150 temporal steps, -0.5 - +9.5 ps

X-state
@7.7eV

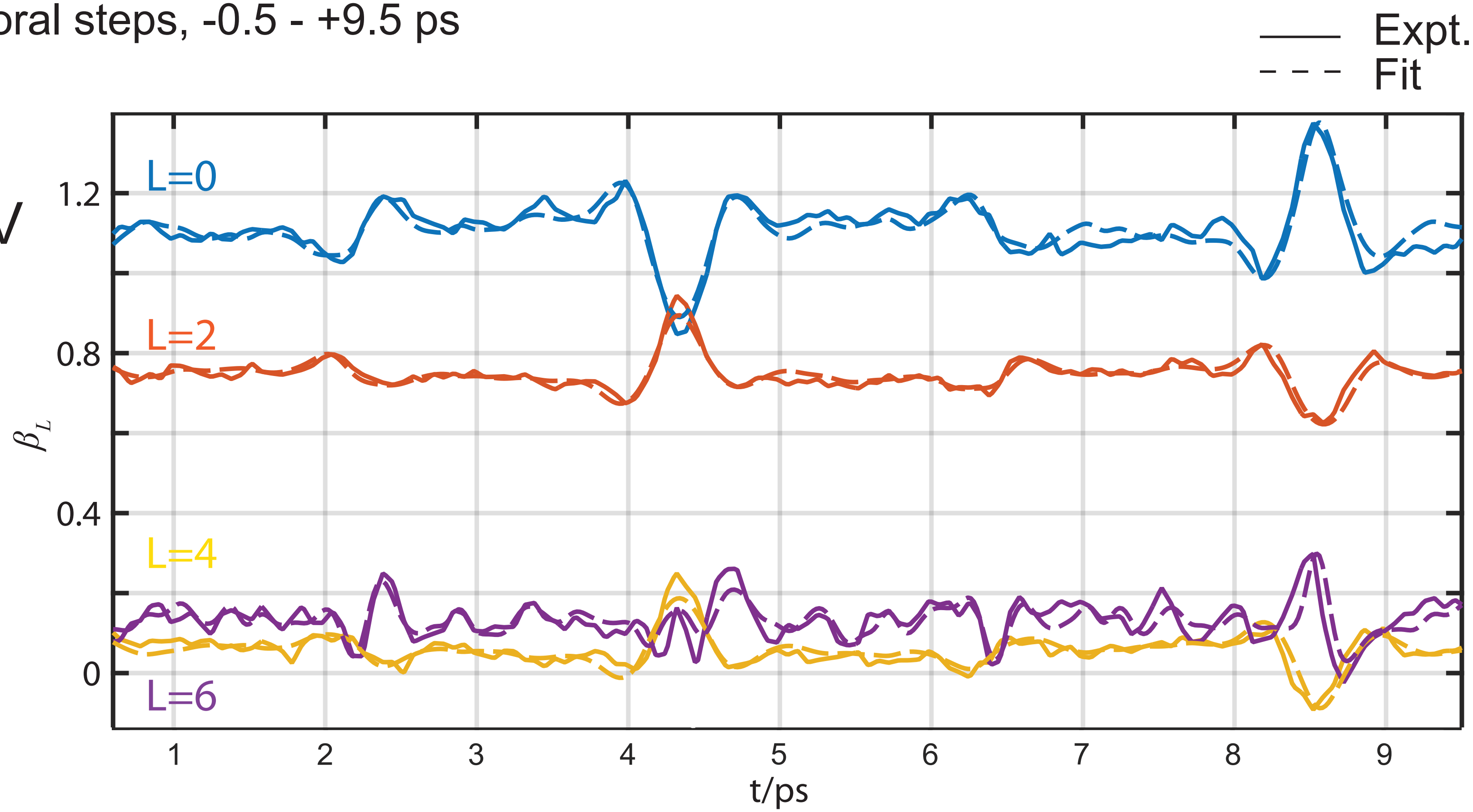

Feature-averaged parameters:

$$\bar{\beta}^{\Gamma}_{L,M}(t) = \bar{\beta}^{\Gamma}_{L,M}(\Delta\bar{k}, t)$$

femtolab.ca

(2): rotational wavepacket retrieval

$$\bar{\beta}^{\Gamma}_{L,M}(t) = \sum_{K,Q} C^{L,M}_{K,Q}(\Gamma) A_{K,-Q}(t)$$

Fit data using simplified form (linear) to determine the rotational wavepacket.

- TDSE calculations of the rotational wavepacket, determines $A_{K,Q}(t)$.
- Best fit to data provides approximation of the wavepacket and conditions (T_{rot}, laser intensity, pulse structure).

↓

T_{rot}=15K, I=20 TWcm^{-2}

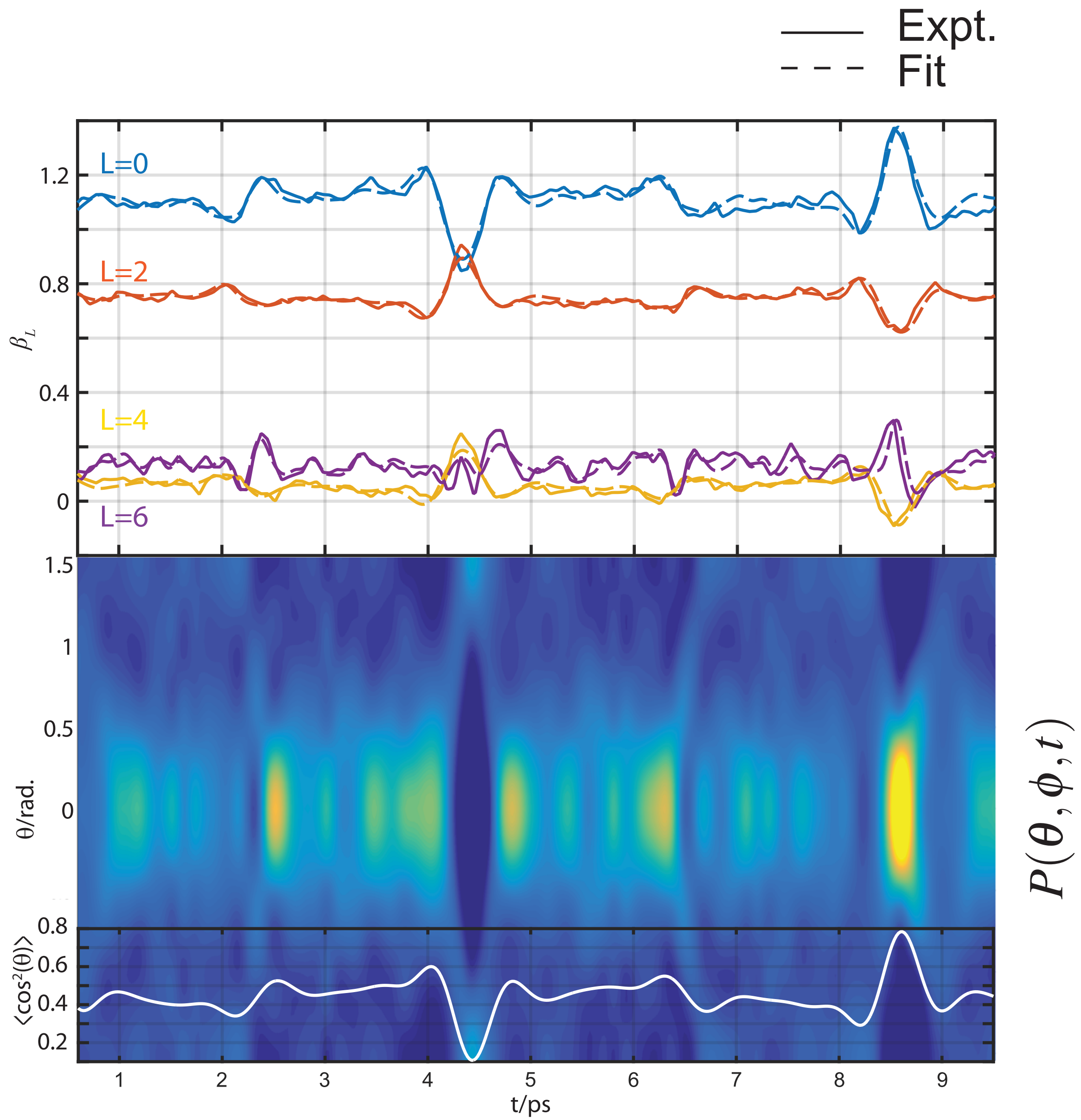

Makhija, V., Ren, X., Gockel, D., Le, A.-T., & Kumarappan, V.
Orientation Resolution through Rotational Coherence Spectroscopy
arXiv 1611.06476 (2016). http://arxiv.org/abs/1611.06476

(3a): photoionization dynamics

$$\bar{\beta}^{\Gamma}_{L,M}(t) = \sum_{K,Q}\left(\sum_{\alpha,\alpha'}\gamma^{\Gamma,\alpha,\alpha'}_{K,Q}\bar{D}^{*}_{\Gamma,\alpha}(\Delta k)\bar{D}_{\Gamma,\alpha'}(\Delta k)\right)A_{K,-Q}(t)$$

Fit data using full form (non-linear) to determine the photoionization dynamics.

- $A_{K,Q}(t)$ from step (2).
- Calculate ang. mom. couplings γ.
- Fit determines (complex) matrix elements $\mathbf{D}_{\alpha}$.

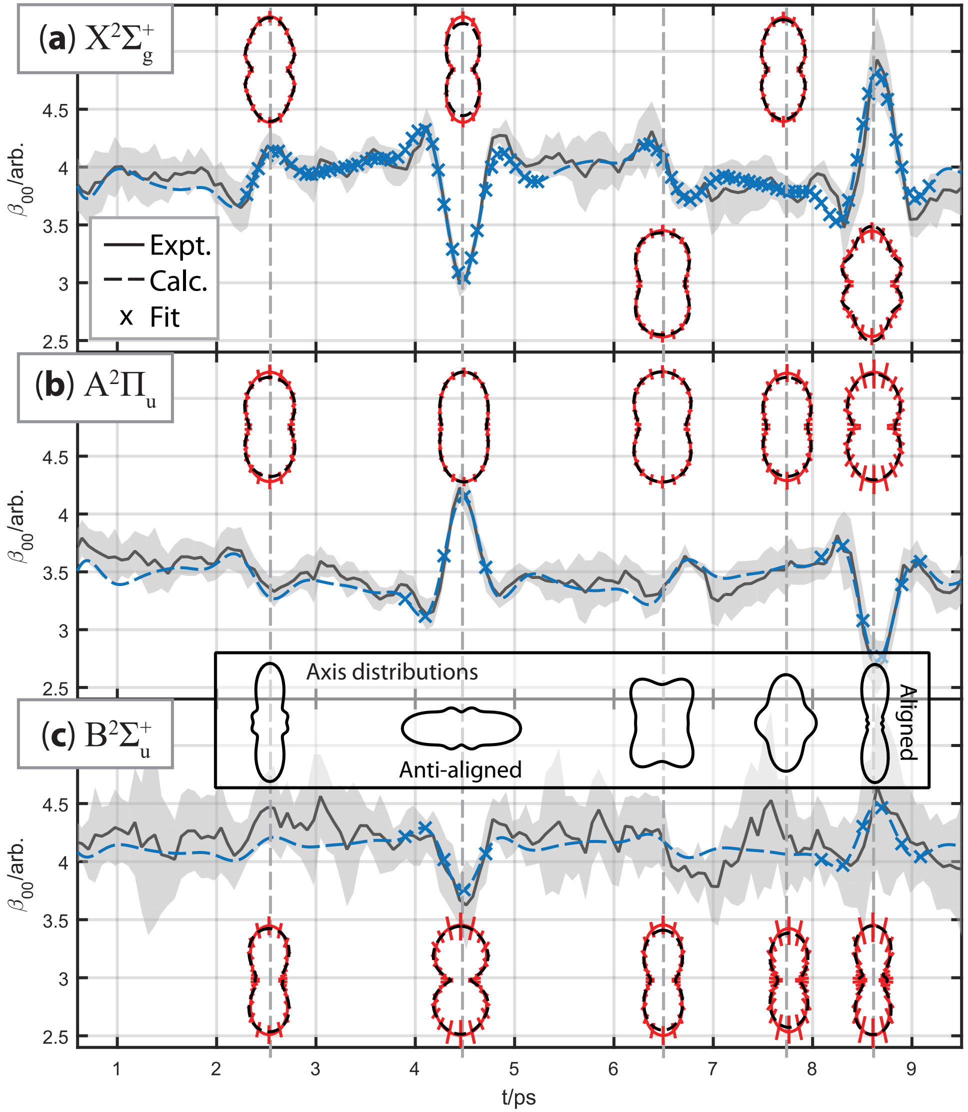

femtolab.ca

(3b): photoionization dynamics

Test fit results for uniqueness & cross-check via

- Statistical sampling
- Additional data

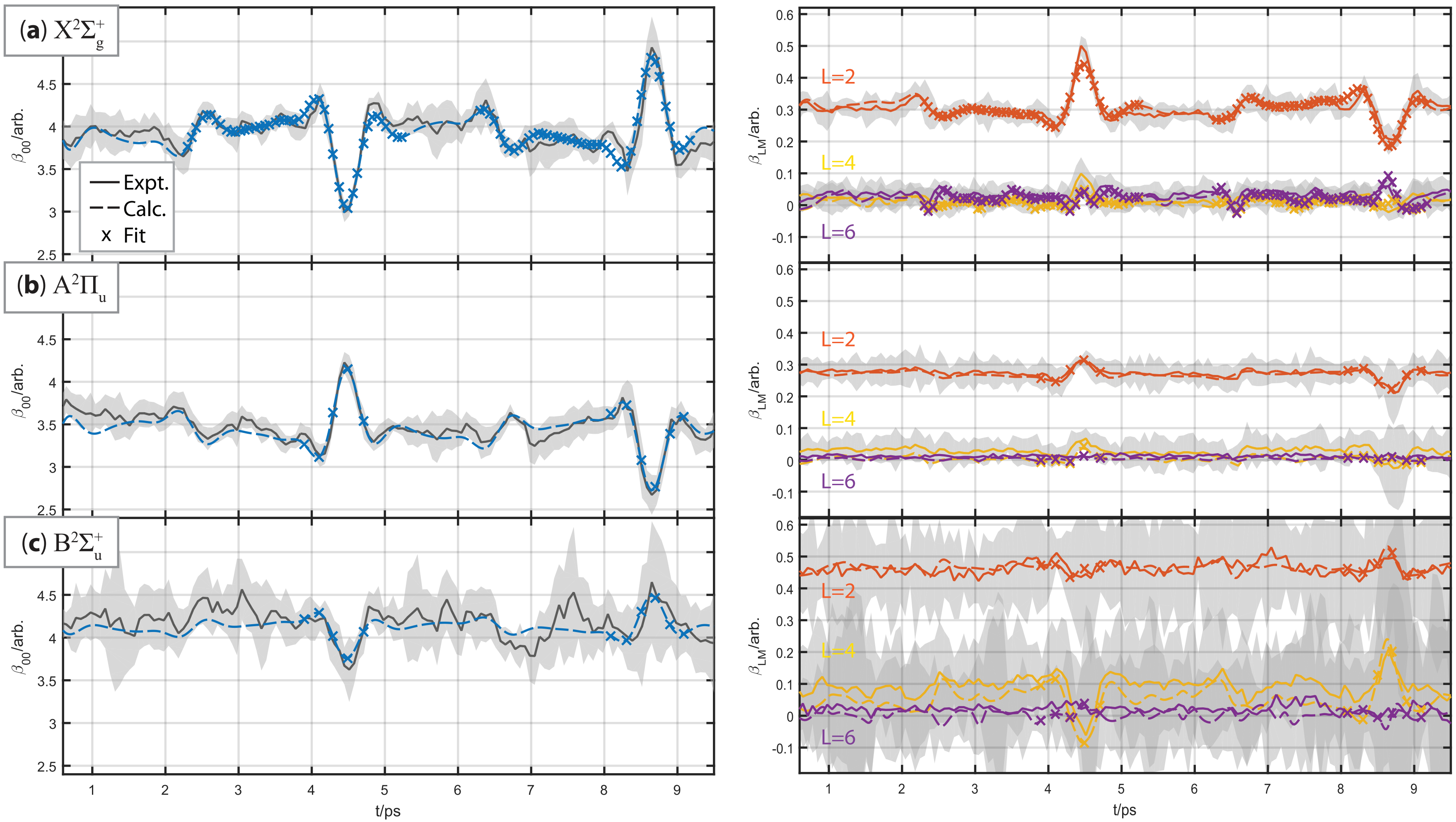

For details see online materials:
https://dx.doi.org/10.6084/m9.figshare.4480349

femtolab.ca

molecular frame reconstruction

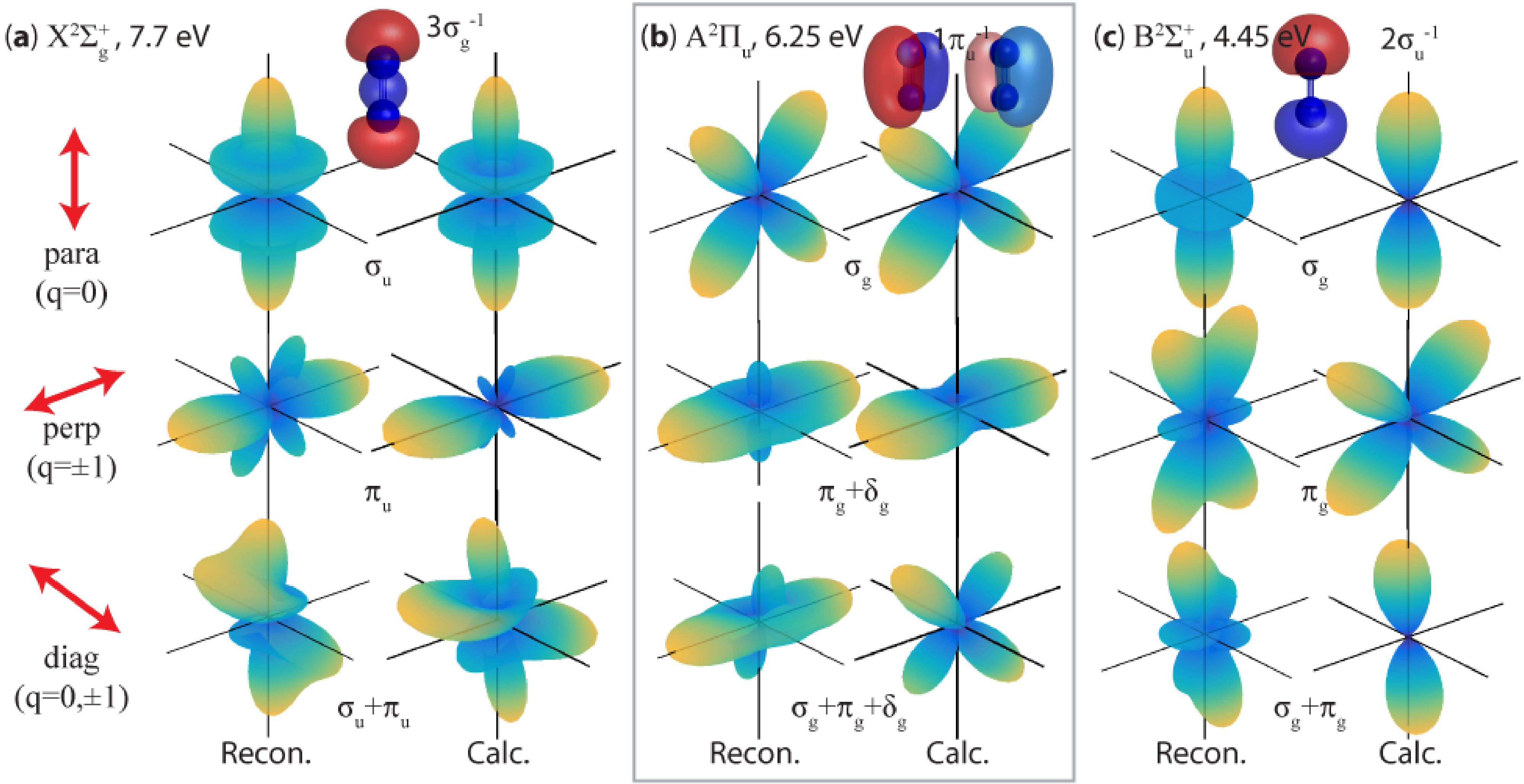

Calculations use bound-free matrix elements from ePolyScat.

http://www.chem.tamu.edu/rgroup/lucchese/ePolyScat.E3.manual/manual.html

femtolab.ca

summary

- Photoelectron metrology
- High information content measurements with rotational wavepacket.
- Bootstrapping analysis protocol:
  - Rotational wavepacket reconstruction.
  - Photoionization dynamics retrieval.
- Demonstrated for N_2, three different energies/final states.
- Molecular frame retrieval from laboratory frame measurements.

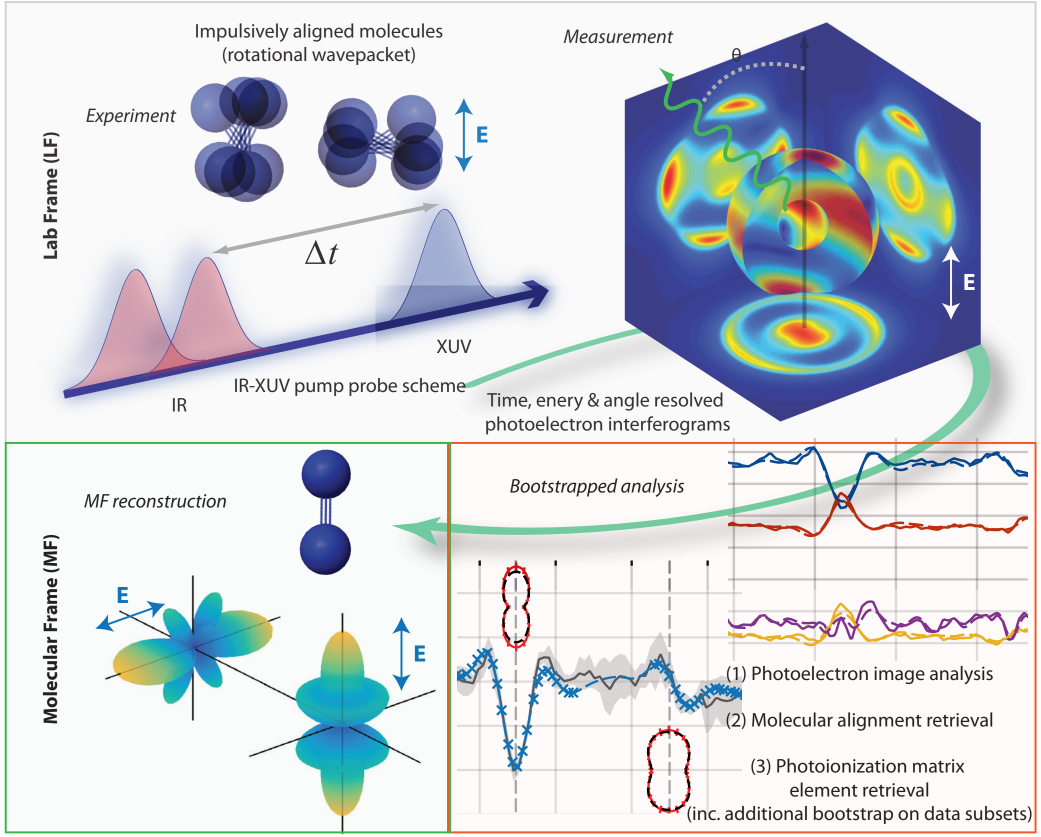

femtolab.ca

outlook

Quantitative photoelectron state reconstruction for "general" molecular photoionization is feasible with rotational wavepacket measurements and bootstrapping protocol...?

OK for symmetric tops... for asymmetric tops much work still to do!

For further discussion, see refs in abstract.

[1] **Molecular Frame Reconstruction Using Time-Domain Photoionization Interferometry.**
Marceau, C., Makhija, V., Platzer, D., Naumov, A. Y., Corkum, P. B., Stolow, A., Villeneuve, D. M., Hockett, P. (2017). Physical Review Letters, 119(8), 83401. http://doi.org/10.1103/PhysRevLett.119.083401

[2] **Coherent control of photoelectron wavepacket angular interferograms.**
Hockett, P., Wollenhaupt, M., & Baumert, T. (2015). Journal of Physics B: Atomic, Molecular and Optical Physics, 48(21), 214004. http://doi.org/10.1088/0953-4075/48/21/214004

[3] **Complete Photoionization Experiments via Ultrafast Coherent Control with Polarization Multiplexing**.
Hockett, P., Wollenhaupt, M., Lux, C., & Baumert, T. (2014). Physical Review Letters, 112(22), 223001. http://doi.org/10.1103/PhysRevLett.112.223001

[4] **Coherent imaging of an attosecond electron wave packet.** (RABBIT based)
Villeneuve, D. M., Hockett, P., Vrakking, M. J. J., & Niikura, H. (2017). Science, 356(6343), 1150–1153. http://doi.org/10.1126/science.aam8393

NRC·CNRC

femtolab.ca

acknowledgements

NRC
Claude Marceau
Varun Makhija
Ruaridh Forbes
Rune Lausten
Albert Stolow
David Villeneuve
Paul Corkum

& everyone else at NRC!

Texas A&M/LBNL
Robert R. Lucchese (ePolyScat)

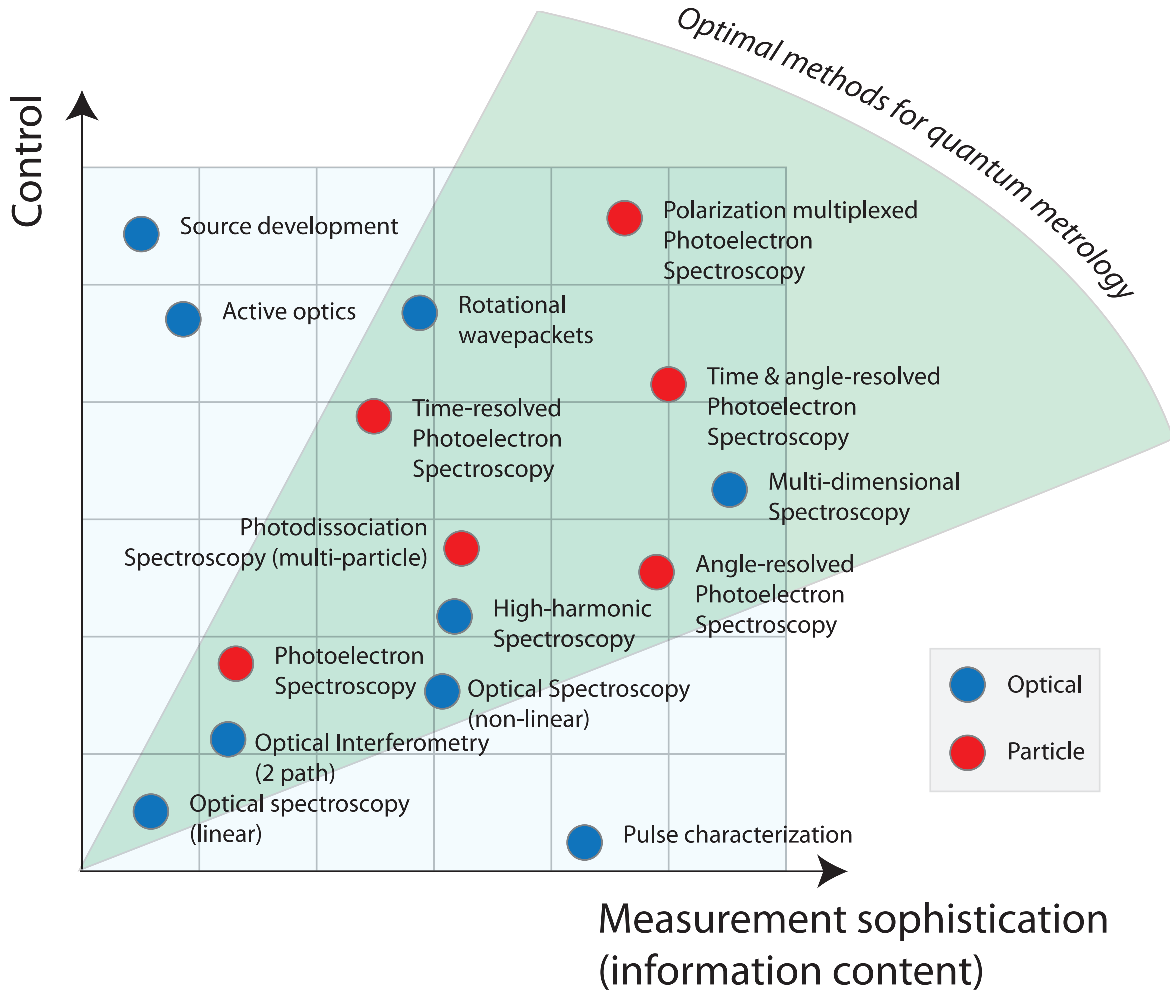

femtolab.ca

for more information...

Slides available via Figshare, DOI: 10.6084/m9.figshare.5645509

arXiv: http://arxiv.org/a/hockett_p_1.html
Figshare: http://figshare.com/authors/Paul_Hockett/100955

Orcid: http://orcid.org/0000-0001-9561-8433
Scholar: https://scholar.google.ca/citations?user=e4FgTYMAAAAJ

Web: www.femtolab.ca

Coming soon:
Quantum Metrology with Photoelectrons
New book for the IOP Concise series, due 2018
https://osf.io/q2v3g/

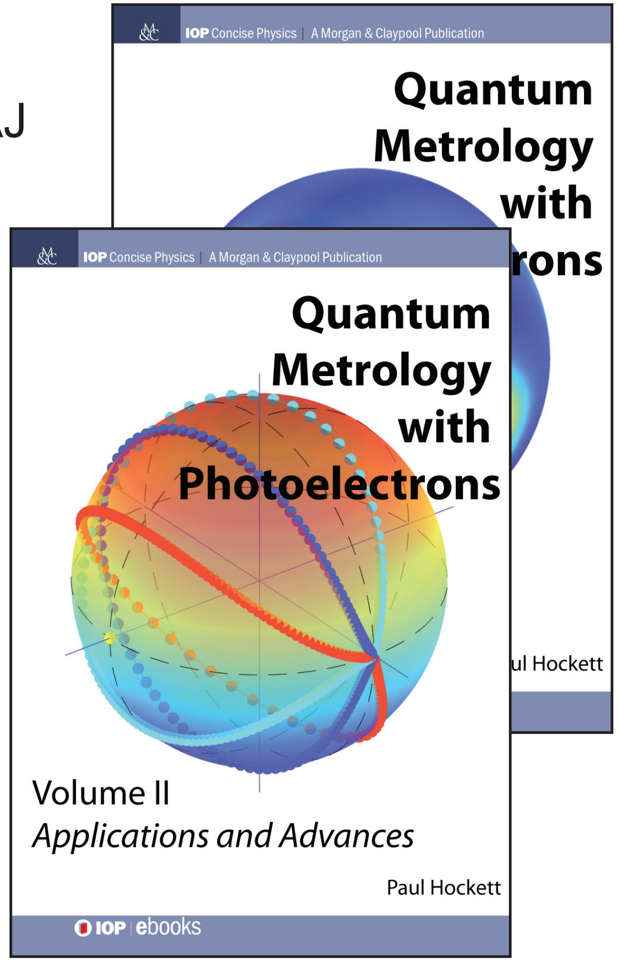

paul.hockett@nrc.ca

femtolab.ca

where are we

NRC, 100 Sussex Drive,
Ottawa, ON, Canada

Web: femtolab.ca

We're always interested in new collaborations and new directions...

If you have an idea, or work that could benefit from our expertise and facilities...

...please get in touch!

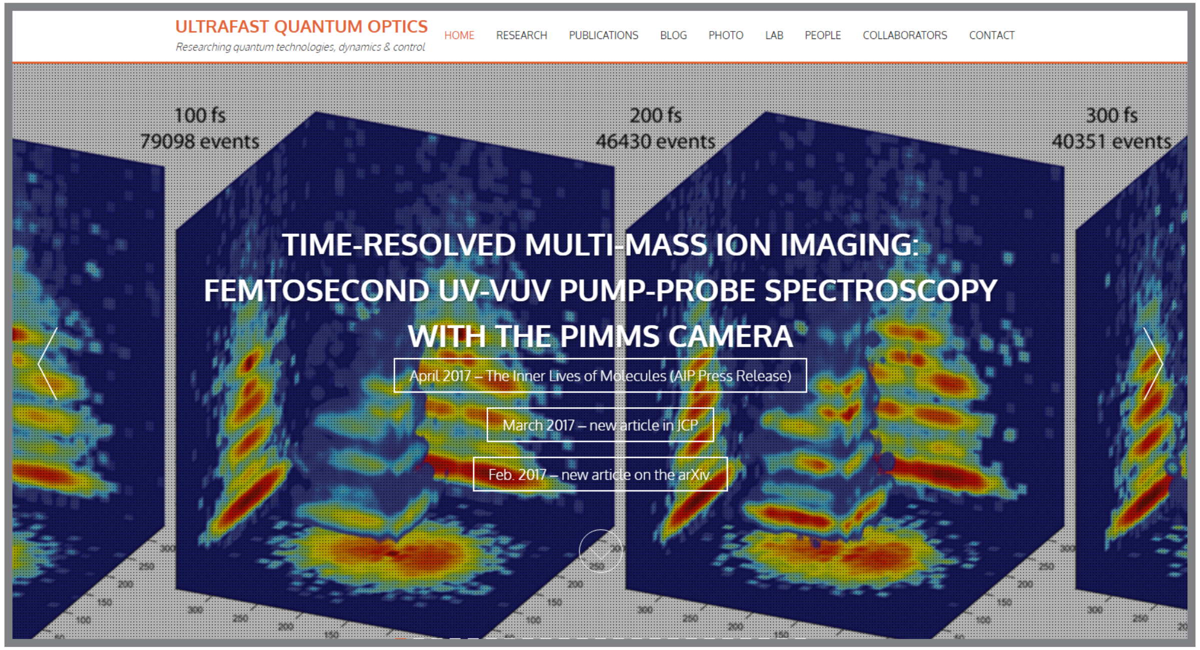

femtolab.ca

N_2 measurements summary

- 267nm driving field
- Two-pulse IR rotational wavepacket preparation
- 150 temporal steps, -0.5 - +9.5 ps

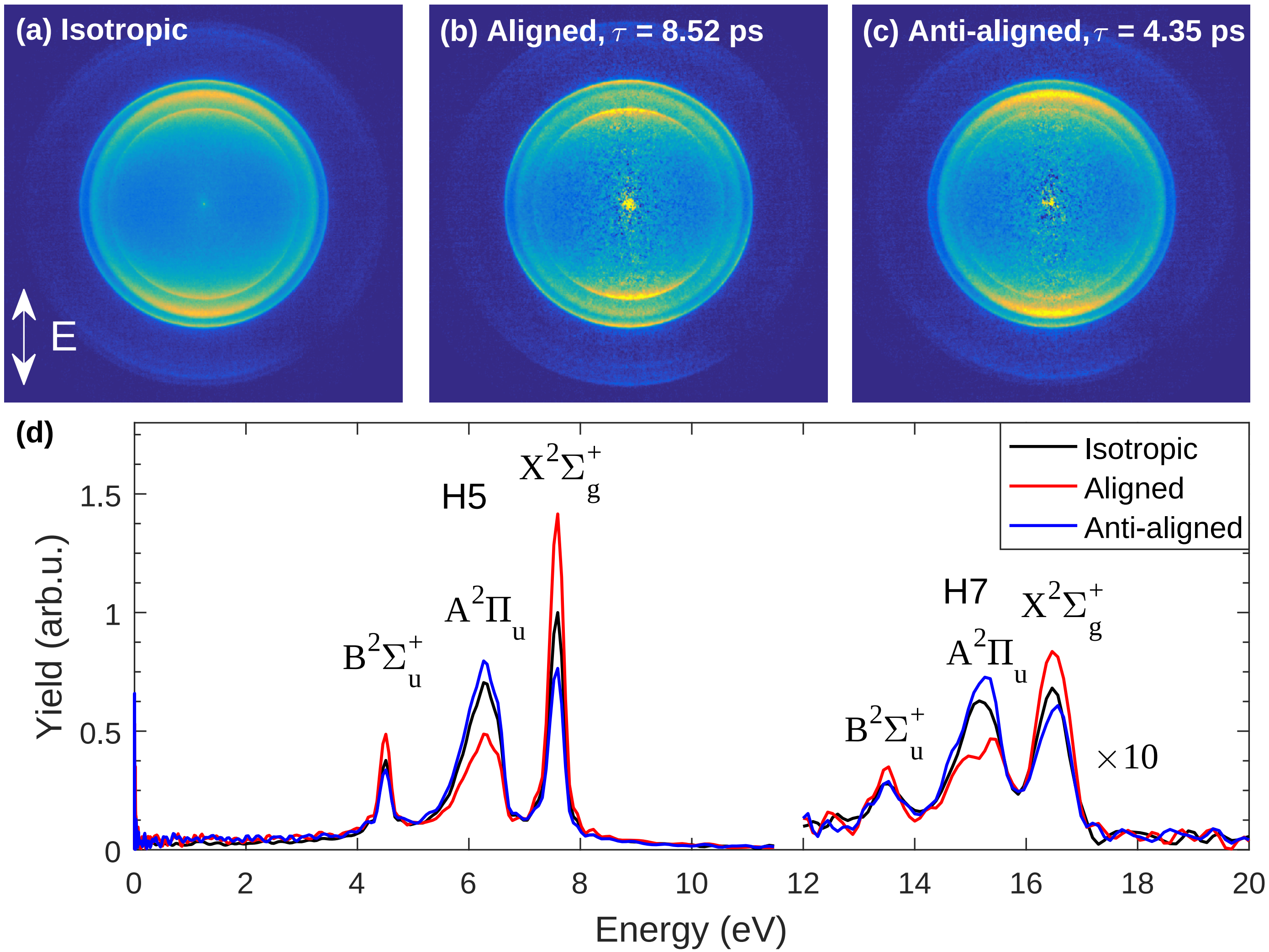

H5 = 23.3 eV H7 = 32.6 eV

femtolab.ca

details: alignement

Notes from Varun's thesis
Laser-induced rotational dynamics as a route to molecular frame measurements
http://krex.k-state.edu/dspace/handle/2097/18522

Determining the alignment Analysis by Varun Makhija

where χ becomes the azimuthal angle of the laser polarization vector. Since the Wigner functions $D^j_{m,k}(\theta,\phi,\chi)$ are an irreducible representation on the rotation group SO(3)[52] the angle dependent ion yield can be expanded as

$$S(\theta,\chi) = \sum_{j,k} C_{j,k} D^j_{0,k}(\theta,\chi), \tag{5.1}$$

$$S(\theta,\chi) = \frac{dW}{d\hat{\Omega}} = \sum_{j,k} C_{j,k} D^j_{0,k}(\theta,\chi),$$

$$C_{j,k} = \sum_{l,m,\lambda,\lambda'} \langle l,-m;l,m|j,0\rangle \langle l,-\lambda;l,\lambda'|j,k\rangle A_{l,\lambda} A_{l,\lambda'} d_{l,m}, \tag{5.5}$$

$$S(t) = \int \rho(\theta,\chi,t) S(\theta,\chi) \sin\theta d\theta d\chi = \sum_{jk} C_{j,k} \int \rho(\theta,\chi,t) D^j_{0k} \sin\theta d\theta d\chi = \sum_{jk} C_{j,k} \left\langle D^j_{0k} \right\rangle (t). \tag{5.7}$$

Measured time-dependent signal

Fitted

Calculated from rotational wavepacket simulations
Function of laser parameters & rotational temperature

https://dx.doi.org/10.6084/m9.figshare.4480349.

details: photoionization

Use known ADMs to determine the unknown dipole matrix elements. Everything else is angular momentum coupling and symmetry parameters; complicated, but analytical.

ADMs from Varun's fit

$$
\begin{aligned}
\boxed{\beta_{L,M}(t)} = {} & (2L+1)^{1/2}\sum_{P}(-1)^{P}\begin{pmatrix} 1 & 1 & P \\ p & -p & R \end{pmatrix} e_{-p}e^{*}_{-p} \\
& \times \sum_{K}\sum_{Q}(2K+1)^{1/2}\begin{pmatrix} P & K & L \\ Q-M & -Q & M \end{pmatrix}\boxed{A_{K,-Q}(t)} \\
& \times \sum_{q,q'}(-1)_{q'}\begin{pmatrix} 1 & 1 & P \\ q & -q' & q'-q \end{pmatrix}\begin{pmatrix} P & K & L \\ q-q' & q'-q & 0 \end{pmatrix} \\
& \times \sum_{l,l'}\sum_{\lambda,\lambda'}(-1)^{\lambda'}(2l+1)^{1/2}(2l'+1)^{1/2}\begin{pmatrix} l & l' & L \\ \lambda & -\lambda' & M \end{pmatrix}\begin{pmatrix} l & l' & L \\ 0 & 0 & 0 \end{pmatrix} \\
& \times (-i)^{l'-l}\sum_{\Gamma,\Gamma'}\sum_{\mu,\mu'}\sum_{h,h'} b^{\Gamma\mu *}_{hl\lambda}\, b^{\Gamma'\mu'}_{h'l'\lambda'} \boxed{\mathbf{D}^{\Gamma\mu *}_{hl}(q)\,\mathbf{D}^{\Gamma'\mu'}_{h'l'}(q')}.
\end{aligned}
$$

(1

Measured angular parameters

Matrix elements to determine

See *General phenomenology of ionization from aligned molecular ensembles* (Hockett, NJP, 17 023069 2015) for details.

https://dx.doi.org/10.6084/m9.figshare.4480349.

details: matrix elements

Γ	q	h	μ	l	m	$\lvert D^{\Gamma\mu}_{hl}(q)\rvert$	$\arg(D^{\Gamma\mu}_{hl}(q))$	$b^{\Gamma\mu}_{hl\lambda}$	Relations
σ_u	0	1	1	1	0	0.53(2)	0*	1	-
				3	0	0.41(2)	1.1(1)	1	-
				5	0	0.49(2)	1.3(4)	1	-
π_u	±1	1	1	1	±1	0.19(3)	-1.4(1)	$1/\sqrt{2}$	$q: D^{\pi_u\mu}_{hl}(+1) = D^{\pi_u\mu}_{hl}(-1)$
				3	±1	0.17(3)	0(1)	$1/\sqrt{2}$	
				5	±1	0.30(2)	-1.6(9)	$1/\sqrt{2}$	

Table 11.1: Symmetrized matrix elements, $X^2\Sigma^+_g$. The sum over all moduli squared are normalized to unity, $\sum\lvert D^{\Gamma\mu}_{hl}(q)/b^{\Gamma\mu}_{hl\lambda}\rvert^2 = 1$. * reference phase, set to zero. Values in parentheses indicate the uncertainty in the final digit.

Γ	q	h	μ	l	m	$\lvert D^{\Gamma\mu}_{hl}(q)\rvert$	$\arg(D^{\Gamma\mu}_{hl}(q))$	$b^{\Gamma\mu}_{hl\lambda}$	Relations
σ_g	±1	1	1,2	0	0	0.58(3)	0*	$1/\sqrt{2}$	$q(\mu=1): D^{\sigma_g 1}_{hl}(+1) = D^{\sigma_g 1}_{hl}(-1)$
									$q(\mu=2): D^{\sigma_g 2}_{hl}(+1) = -D^{\sigma_g 2}_{hl}(-1)$
									$\mu: D^{\sigma_g 2}_{hl}(+1) = \Im[D^{\sigma_g 1}_{hl}(+1)] - i\Re[D^{\sigma_g 1}_{hl}(+1)]$
				2	0	0.23(6)	0.3(12)	$1/\sqrt{2}$	
				4	0	0.15(7)	-0.5(9)	$1/\sqrt{2}$	
δ_g	±1	1	1,2	2	∓2	0.15(7)	-0.5(2)	$1/\sqrt{2}$	$q(\mu=1): D^{\delta_g 1}_{hl}(+1) = D^{\delta_g 1}_{hl}(-1)$
									$q(\mu=2): D^{\delta_g 2}_{hl}(+1) = -D^{\delta_g 2}_{hl}(-1)$
									$\mu: D^{\delta_g 2}_{hl}(+1) = -\Im[D^{\delta_g 1}_{hl}(+1)] + i\Re[D^{\delta_g 1}_{hl}(+1)]$
				4	∓2	0.22(6)	-0.6(8)	$1/\sqrt{2}$	
π_g	0	1,2	1,2	2	±1	0.15(5)	-0.3(30)	$1/\sqrt{2}$	$h(\mu=1): D^{\pi_g 1}_{1l}(0) = D^{\pi_g 1}_{2l}(0)$
									$h(\mu=2): D^{\pi_g 2}_{1l}(0) = -D^{\pi_g 2}_{2l}(0)$
									$\mu: D^{\pi_g 2}_{hl}(0) = \Im[D^{\pi_g 1}_{hl}(0)] - i\Re[D^{\delta_g 1}_{hl}(0)]$
				4	±1	0.05(9)	0.6(30)	$1/\sqrt{2}$	

Table 11.2: Symmetrized matrix elements, $A^2\Pi_u$. The sum over all moduli squared are normalized to unity, $\sum\lvert D^{\Gamma\mu}_{hl}(q)/b^{\Gamma\mu}_{hl\lambda}\rvert^2 = 1$. * reference phase, set to zero. Values in parentheses indicate the uncertainty in the final digit.

Γ	q	h	μ	l	m	$\lvert D^{\Gamma\mu}_{hl}(q)\rvert$	$\arg(D^{\Gamma\mu}_{hl}(q))$	$b^{\Gamma\mu}_{hl\lambda}$	Relations
σ_g	0	1	1	0	0	0.08(21)	0*	1	-
				2	0	0.19(9)	-1.0(13)	1	-
				4	0	0.65(4)	-1.6(19)	1	-
π_g	±1	1	1	2	∓1	0.01(12)	-3.5(35)	$1/\sqrt{2}$	$q: D^{\pi_u\mu}_{hl}(+1) = D^{\pi_u\mu}_{hl}(-1)$
				4	∓1	0.52(3)	0.4(13)		

Table 11.3: Symmetrized matrix elements, $B^2\Sigma^+_u$. The sum over all moduli squared are normalized to unity, $\sum\lvert D^{\Gamma\mu}_{hl}(q)/b^{\Gamma\mu}_{hl\lambda}\rvert^2 = 1$. * reference phase, set to zero. Values in parentheses indicate the uncertainty in the final digit.